THE JOURNAL OF PHYSICAL CHEMISTRY LETTERS
A JOURNAL OF THE AMERICAN CHEMICAL SOCIETY

pubs.acs.org/JPCL

Letter

Hole Dynamics in Photoexcited Hematite Studied with Femtosecond Oxygen K-edge X-ray Absorption Spectroscopy

Yohei Uemura,* Ahmed S. M. Ismail, Sang Han Park, Soonnam Kwon, Minseok Kim, Hebatalla Elnaggar, Federica Frati, Hiroki Wadati, Yasuyuki Hirata, Yujun Zhang, Kohei Yamagami, Susumu Yamamoto, Iwao Matsuda, Ufuk Halisdemir, Gertjan Koster, Christopher Milne, Markus Ammann, Bert M. Weckhuysen, and Frank M. F. de Groot*

Cite This: *J. Phys. Chem. Lett.* 2022, 13, 4207−4214

Read Online

ACCESS | Metrics & More | Article Recommendations | Supporting Information

ABSTRACT: Hematite (α-Fe_2O_3) is a photoelectrode for the water splitting process because of its relatively narrow bandgap and abundance in the earth's crust. In this study, the photoexcited state of a hematite thin film was investigated with femtosecond oxygen K-edge X-ray absorption spectroscopy (XAS) at the PAL-XFEL in order to follow the dynamics of its photoexcited states. The 200 fs decay time of the hole state in the valence band was observed via its corresponding XAS feature.

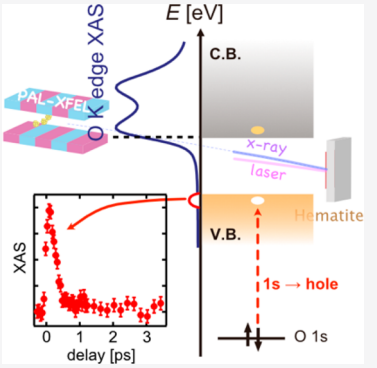

Photochemical water splitting reaction is a key process to generate hydrogen from water without any harmful products. Hematite (α-Fe_2O_3) is one of the promising photoelectrode materials for the solar-assisted water splitting process and has been studied intensively for decades. This is because iron is abundant in the earth's crust,[1] and its optical band gap is in the optimal range of absorption of sunlight.[2,3] α-Fe_2O_3 is also an important photocatalytically active material associated with atmospheric mineral dusts impacting the oxidation capacity of the atmosphere.[4] However, it is known that the intrinsic electronic properties of α-Fe_2O_3 can hinder its catalytic efficiency, in particular for the water splitting reaction. For example, its short hole diffusion length (<4 nm) suppresses the charge separation via electron−hole recombination.[5,6] An in-gap state[7] or a shift of band edge[8] seems to be crucial for such low hole diffusion length. To understand its electronic properties under photoirradiation, theoretical calculations and ultrafast spectroscopic methods have been employed.[3,9−12] It is well-known how the X-ray absorption spectroscopy (XAS) technique can address the element specific electronic structure of materials under investigation, and the recent advances of time-resolved XAS made possible the observation of excited states by photoabsorption in different systems.[10,13−20] In addition, XAS can be obtained under in situ/operando conditions.[21,22] By combining theoretical calculations with XAS experimental data a detailed picture of the local symmetry structure and the electronic states can be obtained.[13,23,24] There have been pioneering works on investigating excited states of metal oxides by optical photoabsorption with the pump−probe XAS methodology.[10,13−20] Furthermore, the birth of X-ray free electron lasers (XFEL) and the developments of X-ray sources by high-harmonic generation (HHG) have extended the scope the pump−probe XAS studies down to femtoseconds.[14,16,25−40] Regarding the photoexcitation of α-Fe_2O_3, the first femtosecond extreme-ultraviolet (XUV) spectroscopic studies on α-Fe_2O_3 thin films were conducted by Vura-Weiss et al.[41] Furthermore, it was suggested by theoretical and experimental XUV studies that localized carriers (small polarons), when being formed, behave as recombination centers, which can contribute to limiting the diffusion length of holes.[9,42−45] We recently demonstrated that different processes occur in the early stage photoexcitation of α-Fe_2O_3 by measuring Fe L_3 XAS and 2p3d resonant inelastic scattering (RIXS) in the Pohang Accelerator Laboratory XFEL (PAL-XFEL).[26] Since the conduction band of α-Fe_2O_3 consists of Fe 3d orbitals mainly, while the valence band comprises O 2p orbitals, Fe L_3 XAS and 2p3d RIXS can probe the conduction band after

Received: January 30, 2022
Accepted: April 5, 2022
Published: May 5, 2022

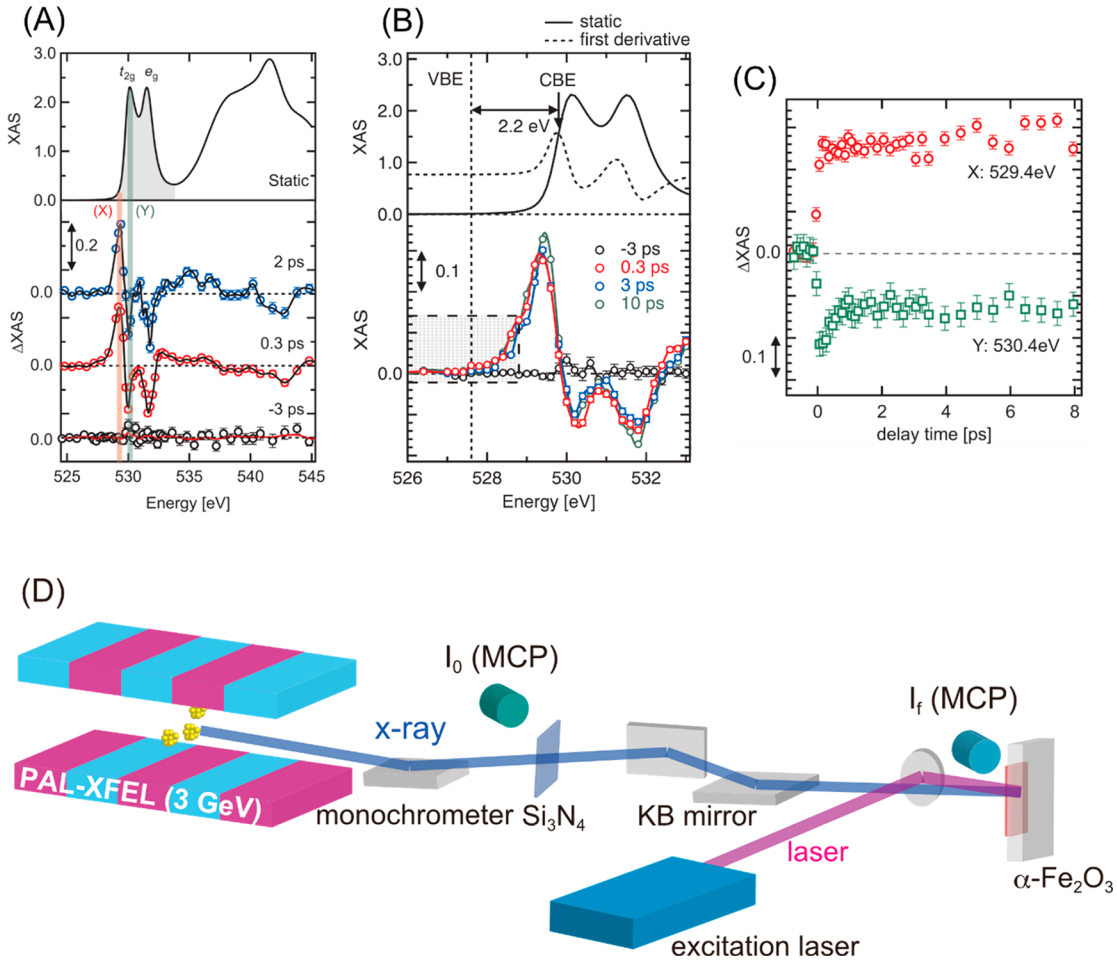

Figure 1. (A) Static oxygen K-edge XAS spectrum of α-Fe_2O_3 measured in SPring-8 (top) and oxygen K-edge ΔXAS of α-Fe_2O_3. Each ΔXAS is the difference between XAS at a delay time of t ps (t = −3, 0.3, or 2 ps) and that at a delay time of −5 ps. (B) O K-edge ΔXAS of α-Fe_2O_3 in the pre-edge region (526−534 eV). (C) Kinetic traces of difference XAS at 529.4 eV (X) and 530.2 eV (Y) shown in panel A. The conduction band edge (CBE) is at 529.8 eV while the valence band edge (VBE) is at 527.6 eV. (D) Illustration of the pump−probe XAS experimental setup in the SSS beamline, PAL-XFEL.

photoexcitation directly. The carrier relaxation and the charge recombination processes were observed from the viewpoint of the electronic state of the Fe 3d orbitals. The changes observed by Fe L_3 XAS and 2p3d RIXS originate from the behavior of excited electrons in the conduction band.

Although previous transient XAS studies on the dynamics of α-Fe_2O_3 used X-ray absorption at Fe, in principle, it should be possible to observe transient features of oxygen XAS in the same time domains (<10 ps) because of its element selectivity. Since the valence band of α-Fe_2O_3 is mainly composed of oxygen 2p orbitals, oxygen K-edge XAS probes the holes in the valence band providing an effective avenue to investigate the dynamics of α-Fe_2O_3 after photoexcitation. Although there has been few reports on femtosecond XAS studies for lighter elements,[46−49] to the best of our knowledge, oxygen K-edge XAS in condensed phases has not been yet investigated in femtoseconds due to the limitation of available X-ray sources and their properties such as X-ray energy, photon flux, and temporal resolution. Herein, we report the ultrafast dynamics of α-Fe_2O_3 as observed by oxygen K-edge XAS for the first time using the state-of-the-art PAL-XFEL.

Oxygen K-edge transient XAS (ΔXAS) spectra of α-Fe_2O_3 are shown in Figure 1A. An illustration of the experimental setup at the soft X-ray scattering and spectroscopy (SSS) beamline at PAL-XFEL is displayed in Figure 1D; a more detailed description of the setup is given in the experimental details section of the Supporting Information. To observe the photoexcited states of α-Fe_2O_3, the 50 nm thin film was excited by a femtosecond laser (wavelength, 400 nm; pulse duration, ∼70 fs). We note that hereafter, *"photoexcited"* state(s), electrons, and holes indicate the excited state, excited electrons, and excited holes, respectively, to avoid confusion. The repetition rate of XFEL was 30 Hz, and the laser was operated at 30 Hz and precisely synchronized with the XFEL. To observe the progress of the photoexcited state, the timing between the X-ray pulse and the laser pulse was changed using an optical delay stage. Each X-ray pulse from the XFEL hit the sample before (i.e., negative delay time) or after (i.e., positive delay time) the sample was excited by a laser pulse. ΔXAS at each delay time (Δt) was calculated as ΔXAS = XAS(Δt) − XAS(−5 ps). Since it required more than 1 h to obtain an XAS spectrum with a good signal-to-noise ratio, the long-term intensity fluctuations can affect the measurements slightly. To minimize this effect, XAS for a desired delay time and the reference XAS (Δt = −5 ps) were measured in sequence, which successfully eliminates artifacts in the transient ΔXAS.[26]

After photoexcitation, there were some distinctive changes observed (ΔXAS for 0.3 and 2 ps), in particular between 528

https://doi.org/10.1021/acs.jpclett.2c00295
J. Phys. Chem. Lett. 2022, 13, 4207−4214

and 533 eV. Compared to the spectral features of the first derivative of the XAS of the ground state, the spectral features of the differential XAS are close to those of the first derivative (Figure S4), which implies that the main differences are attributed to the spectral shift of the O K-edge XAS. The sharp features of the XAS of the ground state (shown as shaded area in the top panel of Figure 1A) originate from electronic transitions from oxygen 1s to 2p orbitals that are hybridized with Fe 3d orbitals. The X-ray absorption features observed between 535 and 545 eV originate from oxygen 2p orbitals which are hybridized with Fe 4s/4p orbitals.[23] In other words, the X-ray absorption between 528 and 533 eV reflects the oxygen p character of the iron 3d band of α-Fe_2O_3, and the absorption intensity between 528 and 533 eV is proportional to the oxygen p-projected density of the unoccupied states.[50] To determine the dynamics of the photoexcited α-Fe_2O_3, the kinetic traces of XAS at the energies of 529.4 eV (denoted as X) and 530.4 eV (denoted as Y) were measured (see Figure 1C). Once the sample was excited by the optical laser, the XAS intensity at 529.4 eV increased while the XAS intensity at 530.4 eV decreased as shown in Figure 1C. These changes correspond to the initial photoexcitation to cause the spectral shift. At longer delay time (>0.2 ps), the XAS intensity at 530.4 eV shows a different trend from the XAS intensity at 529.4 eV. While the XAS intensity at 529.4 eV did not change, that is, no kinetic process was found, the XAS intensity at 530.4 eV decreased by a delay time of 1 ps. The decay process at 530.4 eV was fitted by a single exponential function $f(t) = A + B\exp(-t/\tau)$ (A and B are arbitrary constants), and the time constant τ was estimated as 0.27 ± 0.06 ps.

To observe the behavior of electron holes after photoexcitation, we focused on the pre-edge area below 528.5 eV, that is, below the threshold energy of oxygen K-edge.[51] Figure 2A displays the shaded area of the bottom panel of Figure 1B

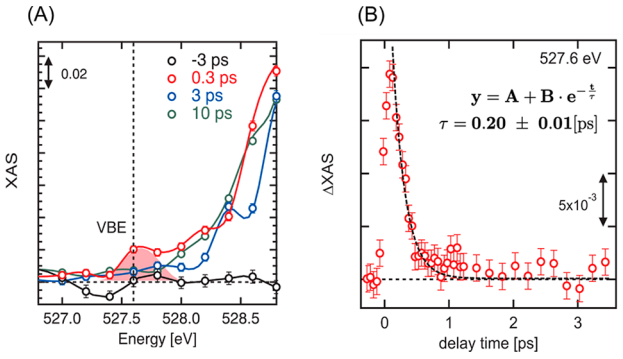

Figure 2. (A) Zoom of the pre-edge region shown as a dashed rectangle in Figure 1B. (B) Kinetic trace of XAS at 527.6 eV shown in Figure 1D. The dashed line is a single exponential function used for fitting.

(526.0−528.8 eV), where the valence band edge (VBE) is expected to be observed. Comparing the transient XAS at a delay time of 0.3 ps with the transient XAS at other delay times, a small increase of XAS was observed around the VBE area, which is a red-shaded area in Figure 2A. Since the XAS intensity is proportional to the density of unoccupied orbitals, the appearance of this peak implies that oxygen 1s electrons will be excited to the unoccupied O 2p orbitals below the energy threshold; that is, the direct electron transition to electron holes in the valence band was observed.

The kinetic trace of XAS at 527.6 eV was also observed (Figure 2B). After the photoexcitation, the XAS intensity rose up immediately and it decreased within 1 ps. The decay process was fitted as a single exponential function, and the time constant was estimated as 0.20 ± 0.01 ps, which is a similar value estimated from the kinetic trace at 530.4 eV (Figure 1C). This result implies that the observed holes in the valence band disappeared within 1 ps by recombination or relaxation processes (we discuss this later in section II).

Hereafter, we would like to discuss the following topics: (I) Transient XAS features above the absorption edge, (II) transient signals below the absorption edge (at 572.6 eV), and (III) the fast kinetic process observed at 529.8 eV.

I. Transient XAS Features above the Absorption Edge. The transient XAS feature shown in Figure 1A is supposed to originate from the formation of Fe(II), which causes the spectral shift in the direction of lower energy. We note that while the L_3 edge XAS of a metal ion shifts in higher energy by approximately 1.5 eV when its valence state changes from 2+ to 3+,[52] the oxygen K-edge XAS of transition metal oxides does not have a general trend. For instance, the oxidation of Fe oxides hardly shifts the oxygen K-edge position in bulk oxides while the oxygen K-edge XAS of Cu and Ni oxides shifts to lower energy upon oxidation.[50,53,54]

After the optical excitation, we identify the following two events: (1) A change in the charge density of Fe atoms that shifts the iron 3d-band energy to lower energies and (2) a decrease of the unoccupied states of the Fe 3d orbitals.

1. A change of the charge density. An initial photoexcited state is created by the optical laser excitation, creating enhanced charge density in the (spin-down) iron 3d-band. The enhanced charge density shifts the iron 3d-band to lower energy, and the oxygen contribution to the iron 3d-band will also shift to lower energy. This effect results in the spectral shift mentioned above.

2. A decrease of the unoccupied state of Fe 3d orbitals. The X-ray absorption between 528 and 533 eV reflects the density of unoccupied Fe 3d orbitals; that is, the X-ray absorption is proportional to (the oxygen character of) the unoccupied Fe 3d orbitals. Since an Fe atom in α-Fe_2O_3 is surrounded by six oxygen atoms (nearly octahedral symmetry), its 3d orbitals are split into two different orbitals groups. The orbitals at the lower energy are t_{2g} orbitals, whereas those at the higher energy are e_g orbitals. The X-ray absorption spectra between 528 and 533 eV shows two peak features, which are assigned to t_{2g} and e_g orbitals, respectively.[50] The energy difference between the t_{2g} and e_g peak corresponds to the crystal field splitting of the 3d orbitals of Fe in α-Fe_2O_3. The splitting in Figure 1A was 1.4 eV which is in agreement with previous reports.[50,51,53] Upon photoexcitation, electrons are excited to the conduction band of α-Fe_2O_3, which is mainly composed by Fe 3d orbitals. In other words, the Fe 3d orbitals are filled by photoexcited electrons so that the X-ray absorption intensity between 528 and 533 eV after photoexcitation decreases.

The photoexcited state undergoes a decay process (~0.2 ps as seen in Figure 1C) and forms a longer lived metastable state. Also, the metastable state has increased charge density with respect to the static Fe^{3+} state. This metastable state could involve reorganization of atoms related to a polaronic state.[44]

https://doi.org/10.1021/acs.jpclett.2c00295
J. Phys. Chem. Lett. 2022, 13, 4207−4214

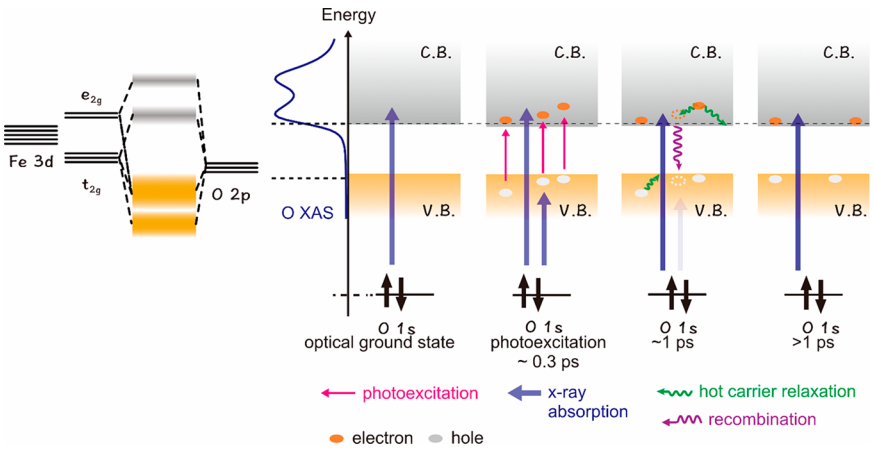

Figure 3. An illustration for the electronic state of the photoexcited α-Fe_2O_3 from the viewpoint of O K-edge XAS. The conduction band is denoted as C.B. and the valence band is as V.B.

II. Transient Signals below the Absorption Edge (at 572.6 eV). Gilbert et al. determined the band edge position of α-Fe_2O_3 from its oxygen K-edge XAS. To determine the edge position of the conduction band, they used the first derivative of the oxygen K-edge XAS, i.e. they defined the conduction band edge (CBE) as the maximum of the first derivative. On the other hand, the VBE position was defined by the first derivative of X-ray emission spectra (XES) of α-Fe_2O_3. According to this definition, they estimated the band gap energy as 2.2 eV, which is in good agreement with a standard value of the band gap of α-Fe_2O_3. We position the VBE by ~2.2 eV below the conduction band edge. In the top panel of Figure 1B, a static oxygen K-edge XAS and its first derivative are displayed. If we calculate the CBE as the maximum of the first derivative, we position it around 529.8 eV. The energy difference between the maximum of the first derivative, that is, the CBE position and the transient peak position shown in Figure 2A is ~2.2 eV, which is in agreement with the band gap value of α-Fe_2O_3. We conclude that the transient peak shown in Figure 2A can be ascribed to the transition of O 1s electrons to O 2p hole states. A similar peak was observed in the oxygen K-edge XAS of a hematite thin film. Braun et al. measured the oxygen K-edge XAS of a photoelectrode consisting of a hematite thin film under photoelectrochemical water splitting reaction, and a small peak appeared 2.2 eV far from the energy threshold.[55] They assigned the peak to an O 2p-type hole.

A fast process with a kinetic constant of 0.2−0.3 ps was reported in the literature.[12,26,41,42,56] This fast process was supposed to be a carrier relaxation, band filling, or band shrinking process. From our results, a fast charge recombination process can be involved in this early stage of photoexcitation. The XAS of the hole state at 527.6 eV disappeared and the line width of the difference signals between 528 and 533 eV did not change. However, since the XAS shifts in lower energy at later delays (>1 ps), there are certain amounts of electrons and holes in the conduction band and the valence band, respectively. We assume that the remaining holes distribute broadly in energy and shift in higher energy. Since the absorption of 1s → 2p excitation can be small and the distribution of the hole states becomes broad, an obvious peak of the hole state was not observed at the longer delays. The absorption of the hole states may be overlapped with the peaks at higher energy, which is another reason why the hole state was not observed at longer delays. The recombination below 1 ps may be affected by the excess carrier density.

III. The Fast Kinetic Process Observed at 529.8 eV. A fast kinetic process with a similar time constant was observed in our previous study of the transient Fe L_3 XAS of the photoexcited α-Fe_2O_3.[26] This fast process was supposed to be a relaxation process of "hot" electrons and holes created by the initial photoexcitation.[11,41,56,57] Since the wavelength of the excitation laser was 400 nm (3.1 eV), which is greater than the bandgap of α-Fe_2O_3, the electrons and holes have excess energy and they relax to the lower energy level releasing their excess energy. The increase of peak Y after 1 ps can be ascribed to a change in hybridization between Fe 3d orbitals and O 2p orbitals driven by the occupation change occurring in the conduction band.

Considering the increase of the peak intensity at 530.4 eV at a delay of 1 ps, the change of the peak intensity can be explained by the decrease of the excited electrons in the t_{2g} orbitals. Since the holes in α-Fe_2O_3 have a limited mobility, a certain number of the holes in the valence band can encounter the electrons and recombine with each other, resulting in a decrease in the population of electrons in the conduction band. Both interpretations seem to be possible for the decay process at 530.4 eV. (It should be noted that a certain amount of electrons and holes exist in the conduction band and the valence band, respectively.)

In summary, the dynamics of the electronic state of the photoexcited α-Fe_2O_3 is illustrated in Figure 3. In the optical ground state, the oxygen K-edge XAS reflects the density of unoccupied Fe 3d orbitals. After the photoexcitation, electrons in the valence band are excited to the conduction band and holes are created in the valence band. The oxygen K-edge spectrum of the photoexcited α-Fe_2O_3 is shifted to lower energy because of the creation of Fe species with excess charge density and change of the hybridization between O 2p orbitals and Fe 3d orbitals. Hot carrier relaxation occurs and the kinetic constant for this process was estimated as ~0.2 ps from the disappearance of the hole states in the valence band and the increase of the XAS intensity for t_{2g} orbitals. In this stage, the hole state disappears as electron−hole recombination, hole's trapping into another energy level, and so on occur. It is supposed that trapped holes/electrons are more likely to be recombined with electrons/holes. The O 2p hole state observed by the transient oxygen K-edge XAS could be

https://doi.org/10.1021/acs.jpclett.2c00295
J. Phys. Chem. Lett. 2022, 13, 4207−4214

trapped hole states; that is, they are distributed in a narrow band in energy and localized in space. In the later delay times (>1 ps), free electrons and holes still exist.

Carnerio et al. observed small polaron formation by a delay time of 1 ps by femtosecond extreme-ultraviolet spectroscopy[44] and we observed a relatively slow dynamics ($t \sim 6$ ps),[26] where the local structure of Fe should change. However, we did not find any signature for these dynamics. This implies that the transient oxygen K-edge XAS reflects the electronics state of Fe 3d orbitals more and the local structural change around the photoexcited Fe atoms does not have much influence on the oxygen K-edge XAS.

We successfully observed transient O K-edge XAS of photoexcited hematite and found several distinctive changes. The main differential spectral feature originates from the formation of Fe(II) species after photoexcitation, and observed dynamics were consistent with our previous study. At 527.6 eV, we found another feature which is associated with the XAS of 1s → 2p hole states and observed a fast decay process. The decay at 527.6 eV suggests the electron−hole recombination can happen below 1 ps. We suppose that the hole states we observed at 527.6 eV are localized in space and energy. At the early state of the photoexcitation, some of the holes can be recombined with electrons within 1 ps.

An advantageous point of pump−probe XAS is the determination of the energy level of carriers against the band edge positions (or absorption edge positions). Using pump−probe XAS can make it possible to figure out the dynamics of photocarriers according to their energy levels. To study more details of the dynamics of α-Fe_2O_3, resonant inelastic X-ray scattering (RIXS) will be helpful.[26,36] Transient RIXS will potentially distinguish energy levels of the conduction band, midgap state, and valence band with an energy resolution of 100 meV (or less). Employing transient soft X-ray absorption spectroscopy can determine the electronic states of elements in metal oxides and reveal the dynamics of photoexcited materials.

EXPERIMENTAL DETAILS

The sample preparation, basic characterization of the sample, and the details of the pump probe experiments at PAL-XFEL are described in the Supporting Information.

ASSOCIATED CONTENT

Supporting Information

The Supporting Information is available free of charge at https://pubs.acs.org/doi/10.1021/acs.jpclett.2c00295.

Sample preparation, basic characterizations of the hematite thin film, the details of the pump−probe setup at PAL-XFEL, the data analysis of X-ray absorption and the evaluation of the temporal resolution at the beamline SSS, PAL-XFEL, and the comparison between transient XAS and the first derivative of the static O K-edge XAS (PDF)

AUTHOR INFORMATION

Corresponding Authors

Yohei Uemura − *Inorganic Chemistry and Catalysis, Debye Institute for Nanomaterials Science, Utrecht University, Utrecht 3584 CG, The Netherlands; Laboratory of Environmental Chemistry, Energy and Environment Research Division, Paul Scherrer Institut, Villigen 5232, Switzerland; European XFEL, Schenefeld 22869, Germany;* orcid.org/0000-0003-3164-7168; Email: yohei.uemura@xfel.eu

Frank M. F. de Groot − *Inorganic Chemistry and Catalysis, Debye Institute for Nanomaterials Science, Utrecht University, Utrecht 3584 CG, The Netherlands;* orcid.org/0000-0002-1340-2186; Email: F.M.F.deGroot@uu.nl

Authors

Ahmed S. M. Ismail − *Inorganic Chemistry and Catalysis, Debye Institute for Nanomaterials Science, Utrecht University, Utrecht 3584 CG, The Netherlands;* orcid.org/0000-0002-2282-1665

Sang Han Park − *PAL-XFEL, Pohang Accelerator Laboratory, Pohang, Gyeongbuk 37673, South Korea*

Soonnam Kwon − *PAL-XFEL, Pohang Accelerator Laboratory, Pohang, Gyeongbuk 37673, South Korea*

Minseok Kim − *PAL-XFEL, Pohang Accelerator Laboratory, Pohang, Gyeongbuk 37673, South Korea*

Hebatalla Elnaggar − *Inorganic Chemistry and Catalysis, Debye Institute for Nanomaterials Science, Utrecht University, Utrecht 3584 CG, The Netherlands;* orcid.org/0000-0002-4223-4054

Federica Frati − *Inorganic Chemistry and Catalysis, Debye Institute for Nanomaterials Science, Utrecht University, Utrecht 3584 CG, The Netherlands*

Hiroki Wadati − *Institute for Solid State Physics, University of Tokyo, Kashiwa, Chiba 277-8581, Japan; Graduate School of Material Science, University of Hyogo, Kamigori, Hyogo 678-1297, Japan*

Yasuyuki Hirata − *Institute for Solid State Physics, University of Tokyo, Kashiwa, Chiba 277-8581, Japan*

Yujun Zhang − *Institute for Solid State Physics, University of Tokyo, Kashiwa, Chiba 277-8581, Japan;* Present Address: Institute of High Energy Physics, Chinese Academy of Sciences Yuquan Road 19B, Shijingshan District, Beijing, 100049, China; orcid.org/0000-0003-4892-1100

Kohei Yamagami − *Institute for Solid State Physics, University of Tokyo, Kashiwa, Chiba 277-8581, Japan*

Susumu Yamamoto − *Institute for Solid State Physics, University of Tokyo, Kashiwa, Chiba 277-8581, Japan;* orcid.org/0000-0002-6116-7993

Iwao Matsuda − *Institute for Solid State Physics, University of Tokyo, Kashiwa, Chiba 277-8581, Japan;* orcid.org/0000-0002-2118-9303

Ufuk Halisdemir − *Faculty of Science and Technology and MESA + Institute for Nanotechnology, University of Twente, Enschede 7500 AE, The Netherlands*

Gertjan Koster − *Faculty of Science and Technology and MESA + Institute for Nanotechnology, University of Twente, Enschede 7500 AE, The Netherlands;* orcid.org/0000-0001-5478-7329

Christopher Milne − *European XFEL, Schenefeld 22869, Germany; SwissFEL, Paul Scherrer Institut, Villigen 5232, Switzerland*

Markus Ammann − *Laboratory of Environmental Chemistry, Energy and Environment Research Division, Paul Scherrer Institut, Villigen 5232, Switzerland;* orcid.org/0000-0001-5922-9000

Bert M. Weckhuysen − *Inorganic Chemistry and Catalysis, Debye Institute for Nanomaterials Science, Utrecht*

https://doi.org/10.1021/acs.jpclett.2c00295
J. Phys. Chem. Lett. 2022, 13, 4207−4214

University, Utrecht 3584 CG, The Netherlands;
orcid.org/0000-0001-5245-1426

Complete contact information is available at:
https://pubs.acs.org/10.1021/acs.jpclett.2c00295

Notes

The authors declare no competing financial interest.

■ ACKNOWLEDGMENTS

This work was financially supported by the European Research Council (ERC) under the European Union's Horizon 2020 research and innovation programme (Grant Agreement No. 340279), Netherlands Center for Multiscale Catalytic Energy Conversion (MCEC), a Gravitation Program from The Netherlands Organisation for Scientific Research (NWO), Grant for collaborative research in Institute for Catalysis, Hokkaido University (18A1005), and a basic science research program funded by the Ministry of Education of Korea (NRF-2020R1A2C1007416 and 2018R1D1A1B07046676). This work was carried out by joint research in the Synchrotron Radiation Research Organization and the Institute for Solid State Physics, the University of Tokyo (Proposal No. 2019A7592). The experiments were performed at SSS end-station of PAL-XFEL (proposal no. 2019-second-SSS-013) funded by the Ministry of Science and ICT of Korea.

■ REFERENCES

(1) Yaroshevsky, A. A. Abundances of chemical elements in the Earth's crust. *Geochem. Int.* **2006**, *44*, 48−55.
(2) Sivula, K.; Le Formal, F.; Grätzel, M. Solar Water Splitting: Progress Using Hematite (α-Fe_2O_3) Photoelectrodes. *ChemSusChem* **2011**, *4*, 432−449.
(3) Tamirat, A. G.; Rick, J.; Dubale, A. A.; Su, W.-N.; Hwang, B.-J. Using hematite for photoelectrochemical water splitting: a review of current progress and challenges. *Nanoscale Horiz.* **2016**, *1*, 243−267.
(4) George, C.; Ammann, M.; D'Anna, B.; Donaldson, D. J.; Nizkorodov, S. A. Heterogeneous Photochemistry in the Atmosphere. *Chem. Rev.* **2015**, *115*, 4218−4258.
(5) Barroso, M.; Pendlebury, S. R.; Cowan, A. J.; Durrant, J. R. Charge carrier trapping, recombination and transfer in hematite (α-Fe_2O_3) water splitting photoanodes. *Chem. Sci.* **2013**, *4*, 2724−2734.
(6) Kay, A.; Cesar, I.; Grätzel, M. New Benchmark for Water Photooxidation by Nanostructured α-Fe_2O_3 Films. *J. Am. Chem. Soc.* **2006**, *128*, 15714−15721.
(7) Klahr, B.; Gimenez, S.; Fabregat-Santiago, F.; Hamann, T.; Bisquert, J. Water Oxidation at Hematite Photoelectrodes: The Role of Surface States. *J. Am. Chem. Soc.* **2012**, *134*, 4294−4302.
(8) Shavorskiy, A.; Ye, X.; Karslıoğlu, O.; Poletayev, A. D.; Hartl, M.; Zegkinoglou, I.; Trotochaud, L.; Nemšák, S.; Schneider, C. M.; Crumlin, E. J.; Axnanda, S.; Liu, Z.; Ross, P. N.; Chueh, W.; Bluhm, H. Direct Mapping of Band Positions in Doped and Undoped Hematite during Photoelectrochemical Water Splitting. *J. Phys. Chem. Lett.* **2017**, *8*, 5579−5586.
(9) Husek, J.; Cirri, A.; Biswas, S.; Baker, L. R. Surface electron dynamics in hematite (α-Fe_2O_3): correlation between ultrafast surface electron trapping and small polaron formation. *Chem. Sci.* **2017**, *8*, 8170−8178.
(10) Hayes, D.; Hadt, R. G.; Emery, J. D.; Cordones, A. A.; Martinson, A. B. F.; Shelby, M. L.; Fransted, K. A.; Dahlberg, P. D.; Hong, J.; Zhang, X.; Kong, Q.; Schoenlein, R. W.; Chen, L. X. Electronic and nuclear contributions to time-resolved optical and X-ray absorption spectra of hematite and insights into photoelectrochemical performance. *Energy Environ. Sci.* **2016**, *9*, 3754−3769.
(11) Sorenson, S.; Driscoll, E.; Haghighat, S.; Dawlaty, J. M. Ultrafast Carrier Dynamics in Hematite Films: The Role of Photoexcited Electrons in the Transient Optical Response. *J. Phys. Chem. C* **2014**, *118*, 23621−23626.
(12) Pendlebury, S. R.; Wang, X.; Le Formal, F.; Cornuz, M.; Kafizas, A.; Tilley, S. D.; Grätzel, M.; Durrant, J. R. Ultrafast Charge Carrier Recombination and Trapping in Hematite Photoanodes under Applied Bias. *J. Am. Chem. Soc.* **2014**, *136*, 9854−9857.
(13) Penfold, T. J.; Szlachetko, J.; Santomauro, F. G.; Britz, A.; Gawelda, W.; Doumy, G.; March, A. M.; Southworth, S. H.; Rittmann, J.; Abela, R.; Chergui, M.; Milne, C. J. Revealing hole trapping in zinc oxide nanoparticles by time-resolved X-ray spectroscopy. *Nat. Commun.* **2018**, *9*, 478.
(14) Uemura, Y.; Kido, D.; Koide, A.; Wakisaka, Y.; Niwa, Y.; Nozawa, S.; Ichiyanagi, K.; Fukaya, R.; Adachi, S.-i.; Katayama, T.; Togashi, T.; Owada, S.; Yabashi, M.; Hatada, K.; Iwase, A.; Kudo, A.; Takakusagi, S.; Yokoyama, T.; Asakura, K. Capturing local structure modulations of photoexcited $BiVO_4$ by ultrafast transient XAFS. *Chem. Commun.* **2017**, *53*, 7314−7317.
(15) Obara, Y.; Ito, H.; Ito, T.; Kurahashi, N.; Thürmer, S.; Tanaka, H.; Katayama, T.; Togashi, T.; Owada, S.; Yamamoto, Y.-I.; Karashima, S.; Nishitani, J.; Yabashi, M.; Suzuki, T.; Misawa, K. Femtosecond time-resolved X-ray absorption spectroscopy of anatase TiO_2 nanoparticles using XFEL. *Struct. Dyn.* **2017**, *4*, 044033.
(16) Uemura, Y.; Kido, D.; Wakisaka, Y.; Uehara, H.; Ohba, T.; Niwa, Y.; Nozawa, S.; Sato, T.; Ichiyanagi, K.; Fukaya, R.; Adachi, S.; Katayama, T.; Togashi, T.; Owada, S.; Ogawa, K.; Yabashi, M.; Hatada, K.; Takakusagi, S.; Yokoyama, T.; Ohtani, B.; Asakura, K. Dynamics of Photoelectrons and Structural Changes of Tungsten Trioxide Observed by Femtosecond Transient XAFS. *Angew. Chem., Int. Ed.* **2016**, *55*, 1364−1367.
(17) Wen, H.; Sassi, M.; Luo, Z.; Adamo, C.; Schlom, D. G.; Rosso, K. M.; Zhang, X. Capturing ultrafast photoinduced local structural distortions of $BiFeO_3$. *Sci. Rep.* **2015**, *5*, 15098.
(18) Santomauro, F. G.; Lübcke, A.; Rittmann, J.; Baldini, E.; Ferrer, A.; Silatani, M.; Zimmermann, P.; Grübel, S.; Johnson, J. A.; Mariager, S. O.; Beaud, P.; Grolimund, D.; Borca, C.; Ingold, G.; Johnson, S. L.; Chergui, M. Femtosecond X-ray absorption study of electron localization in photoexcited anatase TiO_2. *Sci. Rep.* **2015**, *5*, 14834.
(19) Uemura, Y.; Uehara, H.; Niwa, Y.; Nozawa, S.; Sato, T.; Adachi, S.; Ohtani, B.; Takakusagi, S.; Asakura, K. In situ picosecond XAFS study of an excited state of tungsten oxide. *Chem. Lett.* **2014**, *43*, 977−979.
(20) Rittmann-Frank, M. H.; Milne, C. J.; Rittmann, J.; Reinhard, M.; Penfold, T. J.; Chergui, M. Mapping of the Photoinduced Electron Traps in TiO_2 by Picosecond X-ray Absorption Spectroscopy. *Angew. Chem., Int. Ed.* **2014**, *53*, 5858−5862.
(21) Iwasawa, Y.; Asakura, K.; Tada, M. *XAFS Techniques for Catalysts, Nanomaterials, and Surfaces*; Springer International Publishing: 2017.
(22) Van Bokhoven, J. A.; Lamberti, C. *X-Ray Absorption and X-Ray Emission Spectroscopy: Theory and Applications*; John Wiley & Sons: United Kingdom, 2016.
(23) Frati, F.; Hunault, M. O. J. Y.; de Groot, F. M. F. Oxygen K-edge X-ray Absorption Spectra. *Chem. Rev.* **2020**, *120*, 4056.
(24) Penfold, T. J.; Karlsson, S.; Capano, G.; Lima, F. A.; Rittmann, J.; Reinhard, M.; Rittmann-Frank, M. H.; Braem, O.; Baranoff, E.; Abela, R.; Tavernelli, I.; Rothlisberger, U.; Milne, C. J.; Chergui, M. Solvent-Induced Luminescence Quenching: Static and Time-Resolved X-Ray Absorption Spectroscopy of a Copper(I) Phenanthroline Complex. *J. Phys. Chem. A* **2013**, *117*, 4591−4601.
(25) Koide, A.; Uemura, Y.; Kido, D.; Wakisaka, Y.; Takakusagi, S.; Ohtani, B.; Niwa, Y.; Nozawa, S.; Ichiyanagi, K.; Fukaya, R.; Adachi, S.-i.; Katayama, T.; Togashi, T.; Owada, S.; Yabashi, M.; Yamamoto, Y.; Katayama, M.; Hatada, K.; Yokoyama, T.; Asakura, K. Photo-induced anisotropic distortion as the electron trapping site of tungsten trioxide by ultrafast W L1-edge X-ray absorption spectroscopy with full potential multiple scattering calculations. *Phys. Chem. Chem. Phys.* **2020**, *22*, 2615−2621.
(26) Ismail, A. S. M.; Uemura, Y.; Park, S. H.; Kwon, S.; Kim, M.; Elnaggar, H.; Frati, F.; Niwa, Y.; Wadati, H.; Hirata, Y.; Zhang, Y.;

Yamagami, K.; Yamamoto, S.; Matsuda, I.; Halisdemir, U.; Koster, G.; Weckhuysen, B. M.; de Groot, F. M. F. Direct observation of the electronic states of photoexcited hematite with ultrafast 2p3d X-ray absorption spectroscopy and resonant inelastic X-ray scattering. *Phys. Chem. Chem. Phys.* **2020**, *22*, 2685−2692.
(27) Vaz da Cruz, V.; Gel'mukhanov, F.; Eckert, S.; Iannuzzi, M.; Ertan, E.; Pietzsch, A.; Couto, R. C.; Niskanen, J.; Fondell, M.; Dantz, M.; Schmitt, T.; Lu, X.; McNally, D.; Jay, R. M.; Kimberg, V.; Föhlisch, A.; Odelius, M. Probing hydrogen bond strength in liquid water by resonant inelastic X-ray scattering. *Nat. Commun.* **2019**, *10*, 1013.
(28) Norell, J.; Jay, R. M.; Hantschmann, M.; Eckert, S.; Guo, M.; Gaffney, K. J.; Wernet, P.; Lundberg, M.; Föhlisch, A.; Odelius, M. Fingerprints of electronic, spin and structural dynamics from resonant inelastic soft X-ray scattering in transient photo-chemical species. *Phys. Chem. Chem. Phys.* **2018**, *20*, 7243−7253.
(29) Jay, R. M.; Norell, J.; Eckert, S.; Hantschmann, M.; Beye, M.; Kennedy, B.; Quevedo, W.; Schlotter, W. F.; Dakovski, G. L.; Minitti, M. P.; Hoffmann, M. C.; Mitra, A.; Moeller, S. P.; Nordlund, D.; Zhang, W.; Liang, H. W.; Kunnus, K.; Kubicek, K.; Techert, S. A.; Lundberg, M.; Wernet, P.; Gaffney, K.; Odelius, M.; Föhlisch, A. Disentangling Transient Charge Density and Metal-Ligand Covalency in Photoexcited Ferricyanide with Femtosecond Resonant Inelastic Soft X-ray Scattering. *J. Phys. Chem. Lett.* **2018**, *9*, 3538−3543.
(30) Jay, R. M.; Eckert, S.; Fondell, M.; Miedema, P. S.; Norell, J.; Pietzsch, A.; Quevedo, W.; Niskanen, J.; Kunnus, K.; Föhlisch, A. The nature of frontier orbitals under systematic ligand exchange in (pseudo-)octahedral Fe(II) complexes. *Phys. Chem. Chem. Phys.* **2018**, *20*, 27745−27751.
(31) Miller, N. A.; Deb, A.; Alonso-Mori, R.; Garabato, B. D.; Glownia, J. M.; Kiefer, L. M.; Koralek, J.; Sikorski, M.; Spears, K. G.; Wiley, T. E.; Zhu, D.; Kozlowski, P. M.; Kubarych, K. J.; Penner-Hahn, J. E.; Sension, R. J. Polarized XANES Monitors Femtosecond Structural Evolution of Photoexcited Vitamin B12. *J. Am. Chem. Soc.* **2017**, *139*, 1894−1899.
(32) Lemke, H. T.; Kjaer, K. S.; Hartsock, R.; van Driel, T. B.; Chollet, M.; Glownia, J. M.; Song, S.; Zhu, D.; Pace, E.; Matar, S. F.; Nielsen, M. M.; Benfatto, M.; Gaffney, K. J.; Collet, E.; Cammarata, M. Coherent structural trapping through wave packet dispersion during photoinduced spin state switching. *Nat. Commun.* **2017**, *8*, 15342.
(33) Chergui, M.; Collet, E. Photoinduced Structural Dynamics of Molecular Systems Mapped by Time-Resolved X-ray Methods. *Chem. Rev.* **2017**, *117*, 11025−11065.
(34) Shelby, M. L.; Lestrange, P. J.; Jackson, N. E.; Haldrup, K.; Mara, M. W.; Stickrath, A. B.; Zhu, D.; Lemke, H. T.; Chollet, M.; Hoffman, B. M.; Li, X.; Chen, L. X. Ultrafast Excited State Relaxation of a Metalloporphyrin Revealed by Femtosecond X-ray Absorption Spectroscopy. *J. Am. Chem. Soc.* **2016**, *138*, 8752−8764.
(35) Kunnus, K.; Josefsson, I.; Rajkovic, I.; Schreck, S.; Quevedo, W.; Beye, M.; Weniger, C.; Grübel, S.; Scholz, M.; Nordlund, D.; Zhang, W.; Hartsock, R. W.; Gaffney, K. J.; Schlotter, W. F.; Turner, J. J.; Kennedy, B.; Hennies, F.; de Groot, F. M. F.; Techert, S.; Odelius, M.; Wernet, P.; Föhlisch, A. Identification of the dominant photochemical pathways and mechanistic insights to the ultrafast ligand exchange of $Fe(CO)_5$ to $Fe(CO)_4EtOH$. *Struct. Dyn.* **2016**, *3*, 043204.
(36) Wernet, P.; Kunnus, K.; Josefsson, I.; Rajkovic, I.; Quevedo, W.; Beye, M.; Schreck, S.; Grubel, S.; Scholz, M.; Nordlund, D.; Zhang, W.; Hartsock, R. W.; Schlotter, W. F.; Turner, J. J.; Kennedy, B.; Hennies, F.; de Groot, F. M.; Gaffney, K. J.; Techert, S.; Odelius, M.; Fohlisch, A. Orbital-specific mapping of the ligand exchange dynamics of $Fe(CO)_5$ in solution. *Nature* **2015**, *520*, 78−81.
(37) Canton, S. E.; Kjær, K. S.; Vanko, G.; van Driel, T. B.; Adachi, S.-i.; Bordage, A.; Bressler, C.; Chabera, P.; Christensen, M.; Dohn, A. O.; Galler, A.; Gawelda, W.; Gosztola, D.; Haldrup, K.; Harlang, T.; Liu, Y.; Møller, K. B.; Nemeth, Z.; Nozawa, S.; Papai, M.; Sato, T.; Sato, T.; Suarez-Alcantara, K.; Togashi, T.; Tono, K.; Uhlig, J.; Vithanage, D. A.; Warnmark, K.; Yabashi, M.; Zhang, J.; Sundstrom, V.; Nielsen, M. M. Visualizing the non-equilibrium dynamics of photoinduced intramolecular electron transfer with femtosecond X-ray pulses. *Nat. Commun.* **2015**, *6*, 6359.
(38) Kern, J.; Tran, R.; Alonso-Mori, R.; Koroidov, S.; Echols, N.; Hattne, J.; Ibrahim, M.; Gul, S.; Laksmono, H.; Sierra, R. G.; Gildea, R. J.; Han, G.; Hellmich, J.; Lassalle-Kaiser, B.; Chatterjee, R.; Brewster, A. S.; Stan, C. A.; Glöckner, C.; Lampe, A.; DiFiore, D.; Milathianaki, D.; Fry, A. R.; Seibert, M. M.; Koglin, J. E.; Gallo, E.; Uhlig, J.; Sokaras, D.; Weng, T.-C.; Zwart, P. H.; Skinner, D. E.; Bogan, M. J.; Messerschmidt, M.; Glatzel, P.; Williams, G. J.; Boutet, S.; Adams, P. D.; Zouni, A.; Messinger, J.; Sauter, N. K.; Bergmann, U.; Yano, J.; Yachandra, V. K. Taking snapshots of photosynthetic water oxidation using femtosecond X-ray diffraction and spectroscopy. *Nat. Commun.* **2014**, *5*, 4371.
(39) Lemke, H. T.; Bressler, C.; Chen, L. X.; Fritz, D. M.; Gaffney, K. J.; Galler, A.; Gawelda, W.; Haldrup, K.; Hartsock, R. W.; Ihee, H.; Kim, J.; Kim, K. H.; Lee, J. H.; Nielsen, M. M.; Stickrath, A. B.; Zhang, W.; Zhu, D.; Cammarata, M. Femtosecond X-ray Absorption Spectroscopy at a Hard X-ray Free Electron Laser: Application to Spin Crossover Dynamics. *J. Phys. Chem. A* **2013**, *117*, 735−740.
(40) Beye, M.; Sorgenfrei, F.; Schlotter, W. F.; Wurth, W.; Föhlisch, A. The liquid-liquid phase transition in silicon revealed by snapshots of valence electrons. *Proc. Natl. Acad. Sci. U.S.A.* **2010**, *107*, 16772−16776.
(41) Vura-Weis, J.; Jiang, C.-M.; Liu, C.; Gao, H.; Lucas, J. M.; de Groot, F. M. F.; Yang, P.; Alivisatos, A. P.; Leone, S. R. Femtosecond M2,3-Edge Spectroscopy of Transition-Metal Oxides: Photoinduced Oxidation State Change in α-Fe_2O_3. *J. Phys. Chem. Lett.* **2013**, *4*, 3667−3671.
(42) Biswas, S.; Wallentine, S.; Bandaranayake, S.; Baker, L. R. Controlling polaron formation at hematite surfaces by molecular functionalization probed by XUV reflection-absorption spectroscopy. *J. Chem. Phys.* **2019**, *151*, 104701.
(43) Biswas, S.; Husek, J.; Londo, S.; Baker, L. R. Highly Localized Charge Transfer Excitons in Metal Oxide Semiconductors. *Nano Lett.* **2018**, *18*, 1228−1233.
(44) Carneiro, L. M.; Cushing, S. K.; Liu, C.; Su, Y.; Yang, P.; Alivisatos, A. P.; Leone, S. R. Excitation-wavelength-dependent small polaron trapping of photoexcited carriers in α-Fe_2O_3. *Nat. Mater.* **2017**, *16*, 819−825.
(45) Rettie, A. J. E.; Chemelewski, W. D.; Emin, D.; Mullins, C. B. Unravelling Small-Polaron Transport in Metal Oxide Photoelectrodes. *J. Phys. Chem. Lett.* **2016**, *7*, 471−479.
(46) Smith, A. D.; Balčiūnas, T.; Chang, Y.-P.; Schmidt, C.; Zinchenko, K.; Nunes, F. B.; Rossi, E.; Svoboda, V.; Yin, Z.; Wolf, J.-P.; Wörner, H. J. Femtosecond Soft-X-ray Absorption Spectroscopy of Liquids with a Water-Window High-Harmonic Source. *J. Phys. Chem. Lett.* **2020**, *11*, 1981−1988.
(47) Wolf, T. J. A.; Myhre, R. H.; Cryan, J. P.; Coriani, S.; Squibb, R. J.; Battistoni, A.; Berrah, N.; Bostedt, C.; Bucksbaum, P.; Coslovich, G.; Feifel, R.; Gaffney, K. J.; Grilj, J.; Martinez, T. J.; Miyabe, S.; Moeller, S. P.; Mucke, M.; Natan, A.; Obaid, R.; Osipov, T.; Plekan, O.; Wang, S.; Koch, H.; Gühr, M. Probing ultrafast $\pi\pi^*/n\pi^*$ internal conversion in organic chromophores via K-edge resonant absorption. *Nat. Commun.* **2017**, *8*, 29.
(48) Pertot, Y.; Schmidt, C.; Matthews, M.; Chauvet, A.; Huppert, M.; Svoboda, V.; von Conta, A.; Tehlar, A.; Baykusheva, D.; Wolf, J.-P.; Wörner, H. J. Time-resolved x-ray absorption spectroscopy with a water window high-harmonic source. *Science* **2017**, *355*, 264−267.
(49) Attar, A. R.; Bhattacherjee, A.; Pemmaraju, C. D.; Schnorr, K.; Closser, K. D.; Prendergast, D.; Leone, S. R. Femtosecond x-ray spectroscopy of an electrocyclic ring-opening reaction. *Science* **2017**, *356*, 54−59.
(50) de Groot, F. M. F.; Grioni, M.; Fuggle, J. C.; Ghijsen, J.; Sawatzky, G. A.; Petersen, H. Oxygen 1s x-ray-absorption edges of transition-metal oxides. *Phys. Rev. B* **1989**, *40*, 5715−5723.
(51) Gilbert, B.; Frandsen, C.; Maxey, E. R.; Sherman, D. M. Band-gap measurements of bulk and nanoscale hematite by soft x-ray spectroscopy. *Phys. Rev. B* **2009**, *79*, 035108.

https://doi.org/10.1021/acs.jpclett.2c00295
J. Phys. Chem. Lett. 2022, 13, 4207−4214

(52) de Groot, F.; Kotani, A. *Core Level Spectroscopy of Solids*; CRC Press: 2008.
(53) Wu, Z. Y.; Gota, S.; Jollet, F.; Pollak, M.; Gautier-Soyer, M.; Natoli, C. R. Characterization of iron oxides by x-ray absorption at the oxygen K-edgeusing a full multiple-scattering approach. *Phys. Rev. B* **1997**, *55*, 2570−2577.
(54) Colliex, C.; Manoubi, T.; Ortiz, C. Electron-energy-loss-spectroscopy near-edge fine structures in the iron-oxygen system. *Phys. Rev. B* **1991**, *44*, 11402−11411.
(55) Braun, A.; Sivula, K.; Bora, D. K.; Zhu, J.; Zhang, L.; Grätzel, M.; Guo, J.; Constable, E. C. Direct Observation of Two Electron Holes in a Hematite Photoanode during Photoelectrochemical Water Splitting. *J. Phys. Chem. C* **2012**, *116*, 16870−16875.
(56) Joly, A. G.; Williams, J. R.; Chambers, S. A.; Xiong, G.; Hess, W. P.; Laman, D. M. Carrier dynamics in α-Fe2O3 (0001) thin films and single crystals probed by femtosecond transient absorption and reflectivity. *J. Appl. Phys.* **2006**, *99*, 053521.
(57) Cherepy, N. J.; Liston, D. B.; Lovejoy, J. A.; Deng, H.; Zhang, J. Z. Ultrafast Studies of Photoexcited Electron Dynamics in γ- and α-Fe_2O_3 Semiconductor Nanoparticles. *J. Phys. Chem. B* **1998**, *102*, 770−776.

https://doi.org/10.1021/acs.jpclett.2c00295
J. Phys. Chem. Lett. 2022, 13, 4207−4214